

Journal of Mechanics of Materials and Structures

DEVELOPMENT OF FRACTURE MECHANICS MODEL OF
BEAM RETROFITTED WITH CFRP PLATE
SUBJECTED TO CYCLIC LOADING

Shahriar Shahbazpanahi and Hunar Farid Hama Ali

Volume 14, No. 3

May 2019



DEVELOPMENT OF FRACTURE MECHANICS MODEL OF BEAM RETROFITTED WITH CFRP PLATE SUBJECTED TO CYCLIC LOADING

SHAHRIAR SHAHBAZPANAHI AND HUNAR FARID HAMA ALI

A new finite element model was proposed to simulate a concrete beam retrofitted by carbon fiber reinforced polymer (CFRP) composite under cyclic loading. A link element was introduced as interface element to model crack propagation based on the cohesive law in the concrete material. Then the mass and the damping matrix of the link element were defined. A bar element was implemented to simulate the CFRP and then the energy release rates was determined. The load-displacement of the beam was compared with the existing experimental test data and conventional fracture mechanics models carried out using ABAQUS software. The load-displacement curves found by the proposed model were in reasonable agreement with the results of existing experimental data (5.4%–7.6% difference) while conventional fracture mechanics models carried out by the software ABAQUS showed a greater difference (15.2%–24% difference) when compared to the previous experimental tests.

1. Introduction

Fracture mechanics theory is considered to be a more accurate method for predicting crack growth, because this method is similar to the physical reality of crack propagation [Shi 2009]. Two methods are now available for fracture analysis in concrete structures. These can be broadly categorized into linear and nonlinear fracture mechanics. For the first time, linear fracture mechanics was implemented to investigate the crack growth in warships [Esfahani 2007]. In this method, a constant factor was used on the stress around the real crack [Shahbazpanahi 2017]. This constant factor was known as the intensity factor of the stress. The linear fracture mechanics of this theory create stress-singularity in the real crack. Studies such as [Raghu and Renuka 2007; Wu et al. 2011; Pietruszczak and Haghighat 2015], have used linear fracture mechanics to study crack growth. Kaplan [1961] demonstrated that linear fracture mechanics was not able to analyze the crack propagation of concrete beams with normal size [Shi et al. 2001]. Therefore, Hillerborg et al. [1976] presented the crack propagation method on the concrete beam according to nonlinear fracture mechanics. This investigation introduced the fracture region in front of real crack [Fischer and Bohse 2014]. This large and variable region was known as the fracture process zone (FPZ). This zone has the ability to transfer stresses [Shahbazpanahi et al. 2015]. Hence, a study on the role of the FPZ is indispensable for predicting and preventing crack propagation under static loading [Tryding and Ristinmaa 2017]. Although more techniques of the crack propagation have been developed in fracture mechanics, crack modeling for predicting the behavior of concrete structures is still far from satisfactory. Fracture mechanics has been used to simulate crack propagation in the concrete material with softening behavior [Kirane and Bažant 2015; Dong et al. 2016]. Griffith theory can be implemented to

Keywords: ABAQUS, beam, cyclic loading, cohesive, CFRP, propagation.

evaluate the crack growth criterion in the FPZ [Shahbazpanahi 2017]. This theory explains that the energy release rate must be bigger than the critical fracture energy to grow the crack [Ouzaa and Benmansour 2014; Biscaia et al. 2013a]. Based on Griffith theory, for the first time, a cohesive model was suggested to model the FPZ in [Hillerborg et al. 1976]. In the suggested model in [Hillerborg et al. 1976], the stress at the tip of the crack reaches the tensile strength [Dong et al. 2017]. The total area of the stress-opening of the crack is the critical fracture energy. This model was implemented to simulate the crack propagation in normal-size structures. The cohesive model was used in [Dugdale 1960] to study crack propagation in brittle material and by using this method, mesh sensitivity was reduced. Many investigations have been done to improve the cohesive model. The model proposed in [Hillerborg et al. 1976] has been usually implemented because of its practicality and economic considerations [Palmieri and Lorenzis 2014]. Discrete cohesive zone model (DCZM) is one of the most used elements for simulating the cohesive zone. The DCZM was used in some investigations in the review because this model was well-matched with the finite element method [Xie and Waas 2006; Xu et al. 2011; Simon and Kishen 2017]. Also, one of the methods for the crack propagation modeling in the DCZM was the modified crack closure integral method. It can be calculated by the virtual crack closure technique (VCCT). This technique calculates the energy used for closing the crack by multiplying the nodal force and displacement opening. This method is computationally inexpensive and provided satisfactory results [Xie et al. 2006; Xie and Biggers Jr. 2006].

Furthermore, carbon fiber reinforced plastic (CFRP) plate can be used in flexure to prevent flexural crack of a reinforced concrete (RC) beam. Modeling of CFRP retrofitted beams under cyclic loading and investigating of the effect of CFRP plate on the crack propagation criterion in the concrete material is important. Hence, it is necessary to introduce a numerical model to predict the crack propagation of CFRP retrofitted beams under cyclic loading.

A large number of studies on structural behavior of CFRP-strengthened RC beams have recently been reported [Bruno et al. 2013; Carloni and Subramaniam 2013; Abbass et al. 2014; Martinelli and Caggiano 2014; Aravind et al. 2015; Baji et al. 2015]. Many numerical models have been developed for structural analyses of CFRP-strengthened RC beams [Pan and Wu 2014; Zheng et al. 2015; Bruno et al. 2017]. However, most of them are about the analysis of the structural behavior under static loading or the bond-slip of the CFRP. The effects of the CFRP retrofitting on the flexural crack growth criterion under dynamic loading have not been studied based on the literature review.

This paper deals with the accurate stiffness, new mass and damping matrix of the interface element to model the FPZ, material model of the concrete, material model the CFRP plate and new the crack propagation criterion of the flexural-retrofitted RC beam. To obtain the energy release rates in the concrete material, the link element was used. Then, mass and damping matrix of the link element was defined. A bar element was implemented to simulate the CFRP and then the energy dissipation rate by the CFRP was computed. The comparison of the results obtained by proposed model and the available experimental test data were discussed.

2. Methods and materials

In the proposed model, a link elements boundary was used to model crack propagation. The link element defends the softening behavior of the stress-opening of the crack in the submaterial.

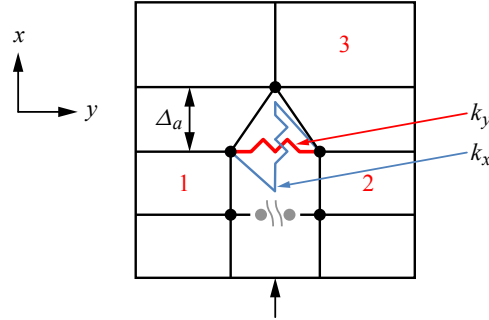


Figure 1. Spring interface element between two nodes.

2.1. Interface element. A nonlinear link is located between two nodes (Figure 1). These nodes are placed in front of crack to model the FPZ. At the beginning of the analysis, the coordinates of joints 1 and 2 are same. The stiffness matrix of the interface element is

$$K = \begin{bmatrix} k_x & 0 & -k_x & 0 \\ 0 & k_y & 0 & -k_y \\ -k_x & 0 & k_x & 0 \\ 0 & -k_y & 0 & k_y \end{bmatrix}, \quad (1)$$

where k_x is normal and k_y is shear stiffness values. In the proposed model, the k_x is obtained from the stress versus crack opening of the concrete material. In this study, k_x and k_y , obtained in [Shahbazpanahi et al. 2012], were used to model the crack softening behavior of subconcrete. The variation of the length of the FPZ was considered to predict the crack propagations.

2.2. Mass matrix and damping matrix in the concrete. Cracks require special modeling if subjected to repeated loading. In the proposed model, the prediction of crack propagation was modeled as subjected to cyclic loading. An improved damping matrix was developed based on the correct stiffness matrix. This damping matrix improves the prediction of the crack propagation subjected to cyclic loading and is more accurate than other existing models. In this study, the mass matrix, M_1 , of the interface element to model crack propagation in concrete is given by

$$M_1 = \frac{1}{2} \rho_1 w_c \begin{bmatrix} 1 & 0 & 0 & 0 \\ 0 & 1 & 0 & 0 \\ 0 & 0 & 1 & 0 \\ 0 & 0 & 0 & 1 \end{bmatrix}, \quad (2)$$

where ρ_1 is mass density of concrete. The Rayleigh damping matrix in concrete, C_1 , is a linear combination of the mass and stiffness matrices, that is,

$$C_1 = \alpha_1 M_1 + \beta_1 K, \quad (3)$$

where α_1 and β_1 are the damping coefficients. These damping coefficients are calculated automatically from modal analysis with initial stiffness by FEAPpv program.

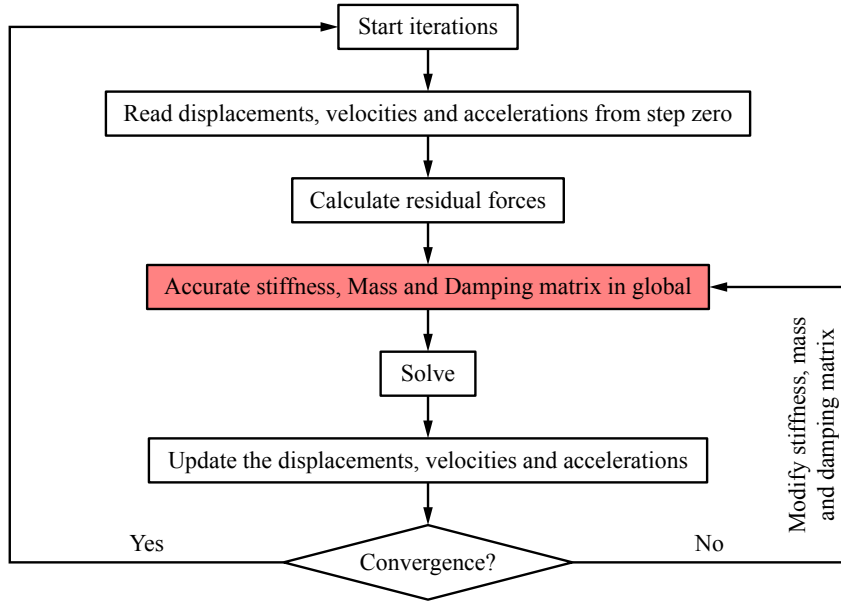


Figure 2. The Newmark's flowchart at each time step.

FEAPpv (Finite Element Analysis Program, Personal Version) was designed for research use [Taylor 2009]. A problem is solved by using a command language concept in FEAPpv. In this program, the solution algorithm is written by the user. Therefore, each user may define a solution strategy that meets specific needs. The system includes sufficient commands that can be used for applications in structural or fluid mechanics, heat transfer, and other areas that require solutions modeled by differential equations, including those for steady-state and transient problems. Users may also add new features for model description and command language statements to meet specific application requirements.

2.3. Time integration. The global equation system is

$$\mathbf{M}\ddot{\mathbf{U}}_t + \mathbf{C}\dot{\mathbf{U}}_t + \mathbf{K}\mathbf{U}_t = \mathbf{F}_t, \quad (4)$$

where \mathbf{M} , \mathbf{K} and \mathbf{C} are the assembled as global mass, stiffness and damping matrices, \mathbf{F}_t is the global load vector, \mathbf{U}_t , $\dot{\mathbf{U}}_t$ and $\ddot{\mathbf{U}}_t$ are the global nodal displacement, nodal velocity and nodal acceleration vectors, respectively. Equation (4) can be solved using standard time integration algorithms. The Newmark method was used in this study to solve dynamic equation. Figure 2 shows the Newmark's flowchart at each time step to solve the dynamic equation.

2.4. Energy release rate in the concrete material. To describe the crack propagation criterion in the fracture process at the crack tip, Griffith energy approach can be used. This approach states that the energy release rate, which is required to form the crack, must be sufficiently larger than the critical fracture energy. The energy release rate is defined as the amount of energy stored in the FPZ [Lee et al. 2010]. Hence, to study the crack state, the crack propagation criterion can be defined in terms of the energy release rate.

Strain energy release rate for the mixed-mode in the concrete was assumed to be the same as Mode I magnitude [Bocca et al. 1991]. Strain energy release rate for Mode I, due to this force, based on VCCT, is

$$G_I = \frac{k_x(u_1 - u_3)^2}{2B\Delta_a}, \quad (5)$$

where Δ_a is mesh size and B is the thickness of the beam. The equation (5) can be applied for mixed-mode and multiple-crack fracture problems. A single-active crack mode strategy following [Shi 2009] is used to simulate multiple cracks. The DCZM element depends on the coordinates of the nodes [Xie and Waas 2006]. Also, u_1 , u_3 and Δ_a depend on the mesh size, however k_x is a material property and it is independent of mesh size. In the results section, mesh-size sensitivity will be done to investigate how results obtained from (5) are mesh-size dependent.

During cyclic loading, the stiffness of concrete was degraded. To determine effective stiffness of concrete under cyclic loading, the stiffness of concrete was proposed as

$$k_N = \left(1 - 0.33 \frac{N}{N_f}\right) k_x, \quad (6)$$

where k_N is the effective stiffness of concrete at N cycles. N_f is the number of loading cycles to failure [Li et al. 2017] and the strain energy release rate at N cycles is

$$G_{I_N} = \frac{k_N(u_1 - u_3)^2}{2B\Delta_a}. \quad (7)$$

2.5. The CFRP effect on flexural crack propagation. The CFRP effect on a flexural crack in the concrete is necessary to prevent growth and improve load bearing. A numerical model based on nonlinear fracture mechanics should be developed to obtain the mechanical response of the CFRP on the FPZ. Let us consider a CFRP reinforced RC beam (see Figure 3). The use of CFRP will increase the rate of energy dissipation and the toughness of concrete structures [Wu and Bailey 2005]. The amount of energy dissipated in the system can be determined by calculating the change in the potential energy of the system. When reloading is applied, the energy dissipation rate of flexural-strengthened members by CFRP is

$$R = \frac{E_F(u_8 - u_{10})(u_{12} - u_{14})}{2b_f L'}, \quad (8)$$

where E_F is the Young's modulus of CFRP, b_f is the width of the CFRP, and u_8 and u_{10} are the displacements in the x direction for nodes 4 and 5, respectively (Figure 3), and u_{12} and u_{14} are the displacements in the x direction for nodes 6 and 7, respectively. L' is the length variation of crack propagation.

Equation (8) is used to estimate the effect of the CFRP as the crack propagates in the concrete beam. This relationship shows that, when the FPZ length increases and the crack opening in concrete is small, the effect of the CFRP on preventing crack propagation is relatively small. Finally, as the FPZ length reaches a constant value and the crack opening increases, the role of the CFRP in resisting crack growth increases. So far, no model has presented a convincing equation for estimating the effect of the CFRP on crack propagation. Given that the CFRP is not located in the crack tip, the rate of energy dissipation due to the moment of the couple caused by the CFRP force is ignored. The energy criterion of crack

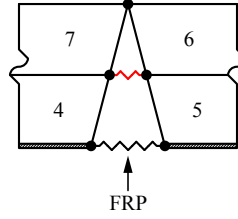


Figure 3. Modeling of flexural strengthened members by CFRP.

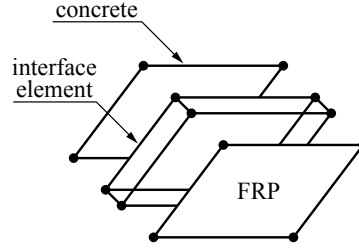


Figure 4. Interface element for modeling bond slip of CFRP.

propagation can be expressed as

$$G_{IN} - R > G_C. \quad (9)$$

Here, R and G_{IN} are based on the size of the mesh. These equations are adopted with the assumption that behavior outside FPZ is linearly elastic. Energy release rate is used to manage convergence in a nonlinear process to a fixed solution. It is assumed that in unloading paths, the effect of the FRP on unloading stiffness is less important and ignored.

2.6. Interface of CFRP bond-slip. Many researchers proposed constitutive models to simulate the bond behavior between an FRP and concrete [Ferracuti et al. 2007; Ko and Sato 2007; Biscaia et al. 2013b]. In this study, a constitutive model was used in [Nakaba et al. 2001]. Figure 4 shows the eight-node interface element for transferring shear in nodal forces between four-node isoparametric quadrilateral element concrete and CFRP elements. In the present study, stress-slip is defined by (10), as used by Nakaba et al.:

$$\frac{\tau}{\tau_{\max}} = \frac{s}{s_{\max}} \cdot \frac{n}{(n+1) + (s/s_{\max})^n}, \quad (10)$$

where τ and s are bond stress and slip between concrete and CFRP, respectively, τ_{\max} is maximum shear stress, s_{\max} is the slip at maximum shear stress and n is a constant.

Two-dimensional plane stress finite elements are applied to analyze crack propagation. The CFRP behavior is elastic but elastic-perfect plastic is considered to model the behavior of steel bars. Four-node isoparametric elements are used for bulk concrete with linear elastic and isotropic behavior. The bar elements are employed to simulate CFRP and longitudinal steel.

material	specifications (mm)	modulus of elasticity (MPa)	compressive strength (MPa)	yield point (MPa)	ultimate tensile strain
concrete	$h = 200, b = 100$	29.45	40.0	–	–
steel	bar dia. = 2×12 mm	$2 \cdot 10^5$	–	415	–
CFRP	$t = 0.13$	$2.40 \cdot 10^5$	–	–	0.00152

Table 1. Material properties of the beam tested in [Kesavan et al. 2013].

3. Results and discussion

In this study, two CFRP-strengthened RC beams are modeled and discussed. The first example is the beam as tested in [Kesavan et al. 2013]. A four-point bending concrete beam strengthened with the CFRP plate on tension face under cyclic loading from that paper was modeled to verify our proposed numerical model. The thickness and width of the CFRP plates were 0.13 mm and 50 mm, respectively. The experimental test results have shown that failure was observed with the debonding of the CFRP plate, and also the model showed that CFRP plate debonding occurred. The CFRP plate increased the bearing capacity by 23% in the proposed model. The material properties of the beam tested in [Kesavan et al. 2013] are summarized in Table 1.

Also, to validate the proposed model, three-dimensional finite element modeling of beams by ABAQUS software was employed. Software, such as ABAQUS, applies linear fracture mechanics to model crack propagation. The proposed model can be compared to the conventional CZM approach used in analysis software such as the FEA software ABAQUS. The beam was modeled by ABAQUS software with 3469 C3D8R elements. An isometric view of the model, cross section of the beam, is shown in Figure 5. The CFRP plate was also set at specific positions to strengthen the beam as shown in Figure 6.

Figure 7 compares the load versus deflection for a beam subjected to cyclic loading obtained by the proposed model, ABAQUS software data and with the results of experimental data in [Kesavan et al. 2013]. Results from the proposed model are in good agreement with those of Kesavan et al. It can be observed that failure load in the proposed model was predicted within 5.4%–7.6% of the experimental data. It can be seen that the push of the curve by the proposed model were similar to the experimental data. However, the push of the curve by the ABAQUS software overestimated the experimental results.

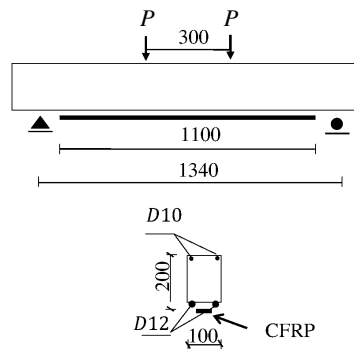


Figure 5. Details and dimensions of the beam strengthened with the CFRP plate tested [Kesavan et al. 2013].

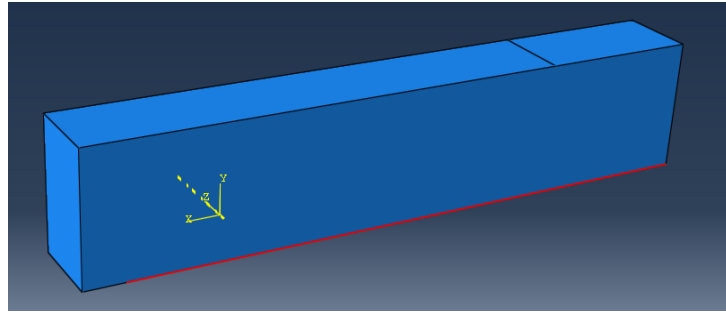


Figure 6. The beam modeled by ABAQUS software.

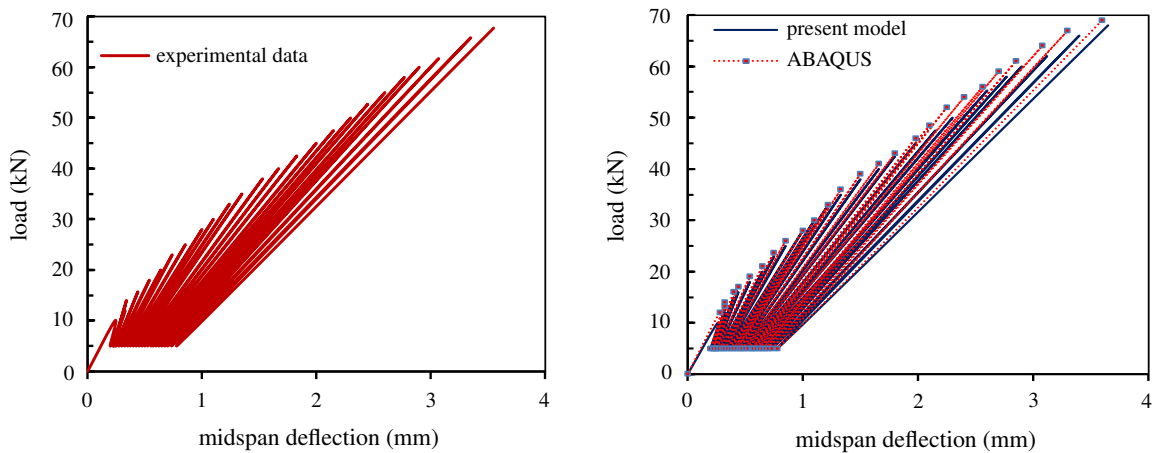


Figure 7. Load-deflection curve: experimental data in [Kesavan et al. 2013] (left) and proposed model and ABAQUS software data (right).

ABAQUS software data shows a greater margin of difference (15.2%–24%) compared to experimental data from [Kesavan et al. 2013].

Figure 8 illustrates the crack pattern of the beam, as modeled. As shown in Figure 8 (left), the flexural

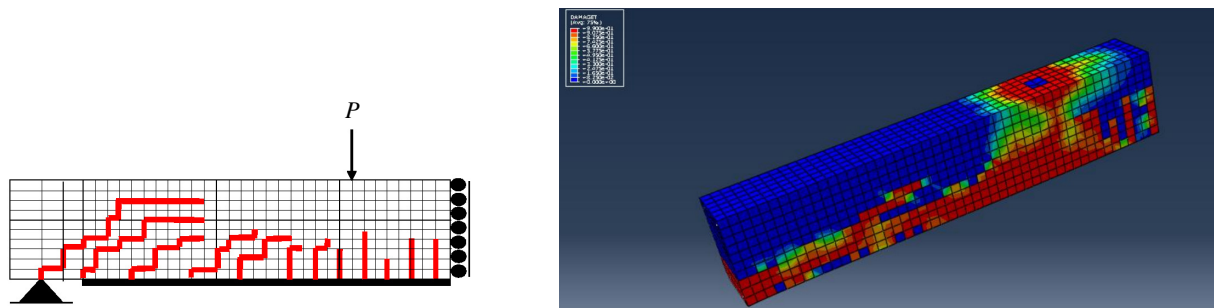


Figure 8. Crack patterns of the beam predicted by the proposed model (left) and ABAQUS (right).

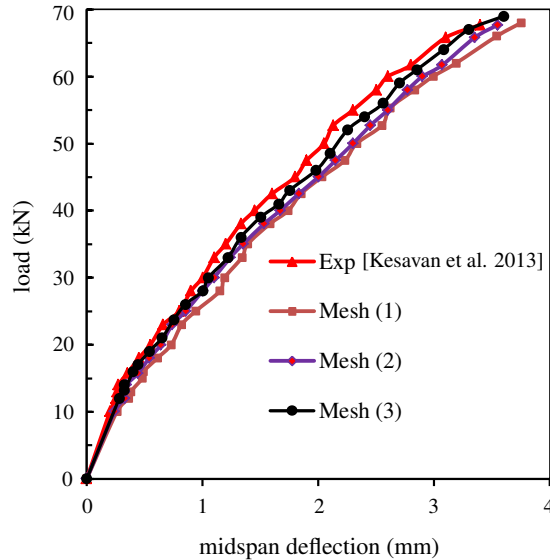


Figure 9. Comparisons pushover of load-deflection between three different meshes.

cracks have not propagated into the upper half of the beam. The proposed model predicted five flexural cracks and five flexural-shear cracks. Within the shear span, the proposed model predicted five flexural-shear cracks compared with two flexural-shear cracks observed in the ABAQUS simulation. However, the flexural-shear cracks intersected together in the ABAQUS software. The number of shear cracks is two in the proposed model compared with one shear crack predicted using ABAQUS. In both cases, shear cracks propagated in the upper half of the beam depth. In the ABAQUS simulation, the real crack is shown in red lines, while the FPZ propagation elements are displayed in green color. It should be noted that the crack path is smooth, but the crack path is illustrated by unconventional lines in this study. In the ABAQUS software, the degradation of the damage is characterized by damage variables from 0 to 0.1. If tensile damage obtained from the software is greater than 0.1, damage occurred. The results from Figure 8 (left) showed that the maximum value of the tensile damage parameter is $0.407 > 0.1$. Therefore, the tensile damage occurred along the red lines as shown in Figure 8 (right). The test showed that failure occurred with the debonding of CFRP plate. However, the model showed that CFRP plate debonding occurs at failure load.

Figure 9 shows the pushover of the load—the midspan deflection with different mesh to study mesh-size sensitivity and to check (5). Mesh 1 had 955 elements (element average size is $18 \text{ mm} \times 16 \text{ mm}$, with a finer mesh of $14 \text{ mm} \times 10 \text{ mm}$). Mesh 2 had 1,344 elements (element average size is $14 \text{ mm} \times 12 \text{ mm}$, with a finer mesh of $12 \text{ mm} \times 8 \text{ mm}$). Mesh 3 had 1,862 elements (element average size is $12 \text{ mm} \times 8 \text{ mm}$, with a finer mesh of $10 \text{ mm} \times 8 \text{ mm}$). The approximate matching of the three curves demonstrates the independence of the model from mesh size and shows that the model exhibited fast convergence. The results in mesh 3 were close to the experimental result (up to 95%).

Another example is a full-scale simply supported beam with four-point load strengthened by the CFRP plate which was tested in [Heffernan and Erki 2004]. A CFRP-strengthened RC beam under a cyclic load as in that article is modeled by using the proposed model. The details of reinforcement

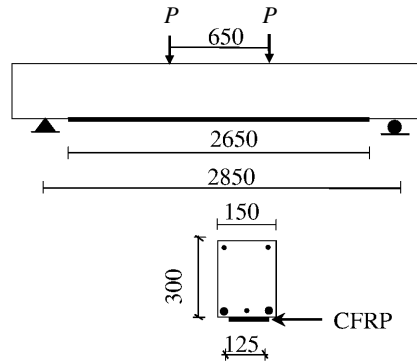


Figure 10. Details of the beam strengthened with the CFRP plate tested in [Heffernan and Erki 2004].

and dimensions of the beam are illustrated in Figure 10. The beam has three longitudinal steel rods of diameter 25.2 mm in tensile side and the compressive side of the RC beam consists of two longitudinal rods of diameter 11.3 mm. The beam span length and width are 2850 mm and 300 mm, respectively. The material properties of this beam are summarized in Table 2.

The critical strain energy for Mode I in concrete and the elastic opening are $0.07 \text{ N} \cdot \text{mm}^{-1}$ and 0.077 mm, respectively. The maximum shear stress between the concrete and the CFRP, and the maximum slip are 5.95 MPa and 0.044 mm, respectively.

The central deflection and number of loading cycles curves observed in the previous experimental test [Heffernan and Erki 2004], the proposed model and the ABAQUS software for the beam strengthened by CFRP are shown in Figure 11. The results of the proposed model are close to that of the experimental results. This finding indicates that the proposed model is validated by the test results. The yield point of the curve in the proposed model is similar to its counterpart in the experimental test results (8%–11% difference). However, this point obtained in the simulations by ABAQUS software is higher than that in the experimental test results (18%–21% difference). The accuracy of the proposed model is also confirmed by the close value of the failure load obtained from the proposed model and the experimental test. The difference in load failure of the beam strengthened by CFRP is 8.4%. Compared with the experimental test, the difference of load failure as analyzed by the ABAQUS software is over-predicted (18%–25% difference).

Figure 12 (left) illustrates an initial mesh and crack paths for the beam by the proposed model at the failure load. The crack pattern predicted by ABAQUS is shown in Figure 12 (right). It can be observed from Figure 12 (left) that five flexural cracks occur at midspan perpendicular to the axis in the beam

material	specifications (mm)	modulus of elasticity (MPa)	compressive strength (MPa)	yield point (MPa)	ultimate tensile strain
concrete	$h = 300, b = 150$	29.45	37.0	–	–
steel	area = 700 mm^2	$2 \cdot 10^5$	–	400	–
CFRP	area = 89.4 mm^2	$2.33 \cdot 10^5$	–	–	0.00175

Table 2. Material properties of the beam tested in [Heffernan and Erki 2004].

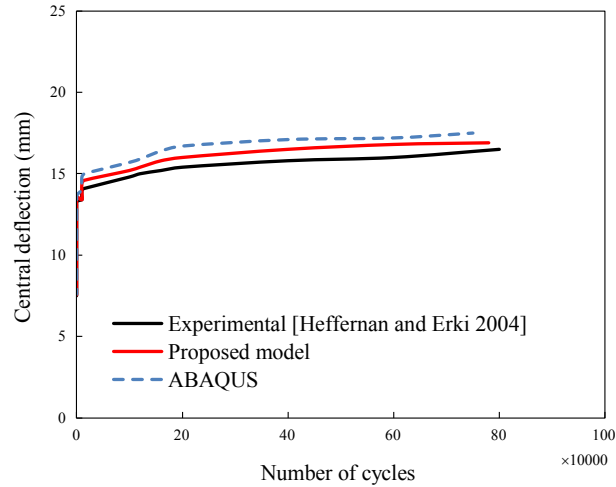


Figure 11. Comparing results for the CFRP-strengthened beam.

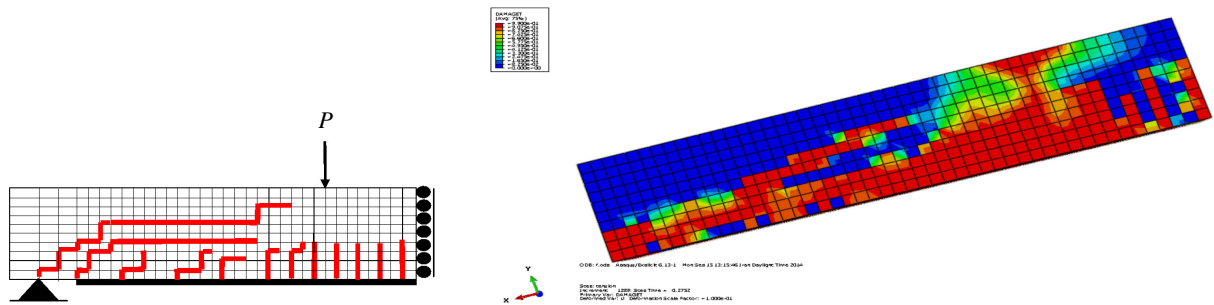


Figure 12. Crack patterns of the beam predicted by the proposed model (left) and ABAQUS (right).

strengthened by CFRP. It is interesting to observe that the crack propagation is controlled by the CFRP plate before into the upper half of the beam. There are five flexural-shear cracks in the shear span of the beam. The two main diagonal shear cracks are formed at the support in the beam. This finding may be compared with the predicted results by ABAQUS software results that only a shear crack was observed in the vicinity of the support shown in Figure 12 (right). The shear cracks grew directly which are followed by a slowly inclining slope towards the loading point. In both the proposed model and ABAQUS software results, there are two shear cracks as shown in Figures 12 (left) and 12 (right), respectively. Crack length was 9.7 mm at 40 kN load in the vicinity of the midspan and 162.7 mm at 120 kN load. Shear cracks started at approximately 180 kN load at the support and expanded upward as load increased.

Based on the proposed model, the effect of CFRP length on the flexural crack propagation is studied. The finding from this parametric study can be used for efficient design of RC beam strengthened by CFRP plate under cyclic loading. The program computed the changing length of CFRP plate while other parameters remained unchanged. Varying lengths of CFRP are 2450 mm, 2550 mm, 2650 mm, 2750 mm and 2850 mm (equal to length of the beam). The influence of the varying lengths of CFRP on the biggest

flexural crack length is shown in Figure 13. As expected, the load capacity increases with the increase length of CFRP plate. It is found that the flexural crack length of the beam strengthened with CFRP decreases with the increase in length of CFRP at the same load. For 2450 mm and 2550 mm lengths of CFRP plate, the crack propagates to the half of the beam while the crack propagation arrests in the beam strengthened by 2650 mm, 2750 mm and 2850 mm lengths. It can be seen that after the crack propagated at a certain point, the load capacity is climbed for 2650 mm, 2750 mm and 2850 mm lengths of CFRP plate. This phenomenon may be due to increase of the slip when the length of CFRP plates increase.

4. Conclusion

A new finite element model was proposed to simulate concrete beam retrofitted by CFRP composite under cyclic loading. A link element was introduced as interface element to model crack propagation based on the cohesive law in the concrete material. Then the mass and the damping matrix of the link element were defined. A bar element was implemented to simulate the CFRP and then the energy release rates was determined. The load-displacement of the beam were compared with the existing experimental test data and conventional fracture mechanics models based on linear fracture mechanics carried out using ABAQUS software. It was observed that the results from the proposed model are in good agreement with the results of previous experimental data (5.4%–7.6% difference). The ABAQUS software data shows a greater difference (15.2%–24% difference) compared to previous experimental test data. The results of the proposed model are close to that of the previous experimental results. This finding indicates that the proposed model was validated by the test results. The yield point of the curve in the proposed model was similar to its counterpart in the experimental test results (8% to 11% difference). However, this point obtained in the simulations by ABAQUS software was higher than that in the experimental test results (18% to 21% difference). The accuracy of the proposed model was also confirmed by the close value of the failure load obtained from the proposed model and the experimental test. The differences of beam with strengthened by CFRP are 8.4% in terms of load failure. Comparing with experimental test, the

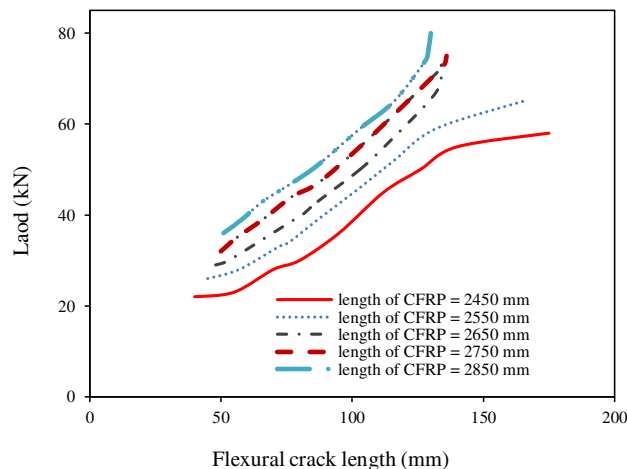


Figure 13. Load vs. largest flexural crack length with different lengths of CFRP plates.

differences of load failure as analyzed via ABAQUS was over-predicted (18% to 25% difference). As expected, the load capacity increases with the increase length of CFRP plate. It is interesting to observe that the crack propagation was controlled with CFRP plate before into the upper half of the beam. In one of the beams, there were five flexural-shear cracks in the shear span of the beam. The two main diagonal shear cracks were formed at the support in the beam. This finding may be compared with the predicted results by ABAQUS software results that only a shear crack was observed in the vicinity of the support. Also, it was found that the flexural crack length of the beam strengthened with CFRP decreases with the increase in length of CFRP at the same load. The mesh-size sensitive analysis demonstrates that the model is independent on mesh size and shows that the model exhibited fast convergence.

References

- [Abbass et al. 2014] M. M. Abbass, V. Matsagar, and A. K. Nagpal, "Bond-slip response of FRP sheets or plates bonded to reinforced concrete beam under dynamic loading", pp. 1959–1969 in *Advances in Structural Engineering*, edited by V. Matsagar, Springer, New Delhi, 2014.
- [Aravind et al. 2015] N. Aravind, A. K. Samanta, D. K. S. Roy, and J. V. Thanikal, "Flexural strengthening of reinforced concrete (RC) beams retrofitted with corrugated glass fiber reinforced polymer (GFRP) laminates", *Curved Layered Struct.* **2**:1 (2015), 244–253.
- [Baji et al. 2015] H. Baji, A. Eslami, and H. R. Ronagh, "Development of a nonlinear FE modelling approach for FRP-strengthened RC beam-column connections", *Structures* **3** (2015), 272–281.
- [Biscaia et al. 2013a] H. C. Biscaia, C. Chastre, and M. A. G. Silva, "Linear and nonlinear analysis of bond-slip models for interfaces between FRP composites and concrete", *Compos. B Eng.* **45**:1 (2013), 1554–1568.
- [Biscaia et al. 2013b] H. C. Biscaia, C. Chastre, and M. A. G. Silva, "Nonlinear numerical analysis of the debonding failure process of FRP-to-concrete interfaces", *Compos. B Eng.* **50** (2013), 210–223.
- [Bocca et al. 1991] P. Bocca, A. Carpinteri, and S. Valente, "Mixed mode fracture of concrete", *Int. J. Solids Struct.* **27**:9 (1991), 1139–1153.
- [Bruno et al. 2013] D. Bruno, F. Greco, and P. Lonetti, "A fracture-ALE formulation to predict dynamic debonding in FRP strengthened concrete beams", *Compos. B Eng.* **46** (2013), 46–60.
- [Bruno et al. 2017] D. Bruno, F. Greco, S. L. Feudo, and P. N. Blasi, "Edge debonding prediction in beams strengthened by FRP composite plates", pp. 105–124 in *Models, simulation, and experimental issues in structural mechanics*, edited by M. Frémond et al., Springer Series in Solid and Structural Mechanics **8**, Springer, 2017.
- [Carloni and Subramaniam 2013] C. Carloni and K. V. Subramaniam, "Investigation of sub-critical fatigue crack growth in FRP/concrete cohesive interface using digital image analysis", *Compos. B Eng.* **51** (2013), 35–43.
- [Dong et al. 2016] W. Dong, D. Yang, X. Zhou, G. Kastiukas, and B. Zhang, "Experimental and numerical investigations on fracture process zone of rock-concrete interface", *Fatigue Fract. Eng. Mater. Struct.* **40**:5 (2016), 820–835.
- [Dong et al. 2017] W. Dong, Z. Wu, X. Zhou, L. Dong, and G. Kastiukas, "FPZ evolution of mixed mode fracture in concrete: experimental and numerical", *Eng. Failure Analysis* **75** (2017), 54–70.
- [Dugdale 1960] D. S. Dugdale, "Yielding of steel sheets containing slits", *J. Mech. Phys. Solids* **8**:2 (1960), 100–104.
- [Esfahani 2007] M. R. Esfahani, *Fracture mechanics of concrete*, Tehran Polytechnic press, Tehran, 2007.
- [Ferracuti et al. 2007] B. Ferracuti, M. Savoia, and C. Mazzotti, "Interface law for FRP-concrete delamination", *Compos. Struct.* **80**:4 (2007), 523–531.
- [Fischer and Bohse 2014] G. Fischer and J. Bohse, "Observation and analysis of fracture processes in concrete with acoustic emission (AE) and digital image correlation (DIC)", pp. 1–8 in *31st Conference of the European Working Group on Acoustic Emission* (Dresden, Germany), 2014.
- [Heffernan and Erki 2004] P. J. Heffernan and M. A. Erki, "Fatigue behavior of reinforced concrete beams strengthened with carbon fiber reinforced plastic laminates", *J. Compos. Constr. (ASCE)* **8**:2 (2004), 132–140.

- [Hillerborg et al. 1976] A. Hillerborg, M. Mod  er, and P.-E. Petersson, "Analysis of crack formation and crack growth in concrete by means of fracture mechanics and finite elements", *Cem. Concr. Res.* **6**:6 (1976), 773–781.
- [Kaplan 1961] M. Kaplan, "Crack propagation and the fracture concrete", *ACI J.* **58**:11 (1961), 591–610.
- [Kesavan et al. 2013] K. Kesavan, K. Ravisankar, R. Senthil, and A. K. F. Ahmed, "Experimental studies on performance of reinforced concrete beam strengthened with CFRP under cyclic loading using FBG array", *Measurement* **46**:10 (2013), 3855–3862.
- [Kirane and Ba  ant 2015] K. Kirane and Z. P. Ba  ant, "Size effect in Paris law for quasibrittle materials analyzed by the microplane constitutive model M7", *Mech. Res. Commun.* **68** (2015), 60–64.
- [Ko and Sato 2007] H. Ko and Y. Sato, "Bond stress-slip relationship between FRP sheet and concrete under cyclic load", *J. Compos. Constr. (ASCE)* **11**:7 (2007), 419–426.
- [Lee et al. 2010] J. H. Lee, R. M. Chacko, and M. M. Lopez, "Use of mixed-mode fracture interfaces for the modeling of large-scale FRP-strengthened beams", *J. Compos. Constr. (ASCE)* **14**:6 (2010), 845–855.
- [Li et al. 2017] D. Li, P. Huang, X. Guo, X. Zheng, J. Lin, and Z. Chen, "Fatigue crack propagation behavior of RC beams strengthened with CFRP under cyclic bending loads", *Fatigue Fract. Eng. Mater. Struct.* **41**:1 (2017), 212–222.
- [Martinelli and Caggiano 2014] E. Martinelli and A. Caggiano, "A unified theoretical model for the monotonic and cyclic response of FRP strips glued to concrete", *Polymers* **6**:2 (2014), 370–381.
- [Nakaba et al. 2001] K. Nakaba, K. K., T. Furuta, and K. Yoshizawa, "Bond behavior between fiber-reinforced polymer laminates and concrete", *ACI Struct. J.* **98**:3 (2001), 359–367.
- [Ouzaa and Benmansour 2014] K. Ouzaa and M. B. Benmansour, "Cracks in continuously reinforced concrete pavement", *Arab. J. Sci. Eng.* **39**:12 (2014), 8593–8608.
- [Palmieri and Lorenzis 2014] V. Palmieri and L. D. Lorenzis, "Multiscale modeling of concrete and of the FRP-concrete interface", *Eng. Fract. Mech.* **131** (2014), 150–175.
- [Pan and Wu 2014] J. Pan and Y.-F. Wu, "Analytical modeling of bond behavior between FRP plate and concrete", *Compos. B Eng.* **61** (2014), 17–25.
- [Pietruszczak and Haghghat 2015] S. Pietruszczak and E. Haghghat, "Modeling of fracture propagation in concrete structures using a constitutive relation with embedded discontinuity", *Studia Geotechnica et Mechanica* **36**:4 (2015), 27–33.
- [Raghu and Renuka 2007] P. B. K. Raghu and D. M. V. Renuka, "Extension of FCM to plain concrete beams with vertical tortuous cracks", *Eng. Fract. Mech.* **74**:17 (2007), 2758–2769.
- [Shahbazpanahi 2017] S. Shahbazpanahi, "Mechanical analysis of a shear-cracked RC beam", *Acta Scientiarum. Technol.* **39**:3 (2017), 285–290.
- [Shahbazpanahi et al. 2012] S. Shahbazpanahi, A. A. A. Ali, F. N. Aznieta, and A. Kamgar, "A simple method to model crack propagation in concrete", *Constructii J.* **13**:1 (2012), 41–50.
- [Shahbazpanahi et al. 2015] S. Shahbazpanahi, A. A. A. Ali, A. Kamgar, and N. Farzadnia, "Fracture mechanic modeling of fiber reinforced polymer shear-strengthened reinforced concrete beam", *Compos. B Eng.* **68** (2015), 113–120.
- [Shi 2009] Z. Shi, *Crack analysis in structural concrete: theory and applications*, Butterworth-Heinemann, Burlington, USA, 2009.
- [Shi et al. 2001] Z. Shi, M. Ohtsu, M. Suzuki, and Y. Hibino, "Numerical analysis of multiple cracks in concrete using the discrete approach", *J. Struct. Eng. (ASCE)* **127**:9 (2001), 1085–1091.
- [Simon and Kishen 2017] K. M. Simon and J. M. C. Kishen, "A multiscale approach for modeling fatigue crack growth in concrete", *Int. J. Fatigue* **98** (2017), 1–13.
- [Taylor 2009] L. R. Taylor, *FEAPpv source: a finite element analysis program*, University of California, Berkeley, 2009.
- [Tryding and Ristinmaa 2017] J. Tryding and M. Ristinmaa, "Normalization of cohesive laws for quasi-brittle materials", *Eng. Fract. Mech.* **178** (2017), 333–345.
- [Wu and Bailey 2005] Z. J. Wu and C. G. Bailey, "Fracture resistance of a cracked concrete beam post-strengthened with FRP sheets", *Int. J. Fract.* **135** (2005), 35–49.
- [Wu et al. 2011] Z. Wu, H. Rong, J. Zheng, F. Xu, and W. Dong, "An experimental investigation on the FPZ properties in concrete using digital image correlation technique", *Eng. Fract. Mech.* **78**:17 (2011), 2978–2990.

- [Xie and Biggers Jr. 2006] D. Xie and S. B. Biggers Jr., “Progressive crack growth analysis using interface element based on the virtual crack closure technique”, *Finite Elem. Anal. Des.* **42**:11 (2006), 977–984.
- [Xie and Waas 2006] D. Xie and A. M. Waas, “Discrete cohesive zone model for mixed-mode fracture using finite element analysis”, *Eng. Fract. Mech.* **73**:13 (2006), 1783–1796.
- [Xie et al. 2006] D. Xie, A. G. Salvi, C. Sun, A. M. Waas, and A. Caliskan, “Discrete cohesive zone model to simulate static fracture in 2D triaxially braided carbon fiber composites”, *J. Compos. Mater.* **40**:22 (2006), 2025–2046.
- [Xu et al. 2011] F. Xu, Z. Wu, J. Zheng, Y. Zhao, and K. Liu, “Crack extension resistance curve of concrete considering variation of FPZ length”, *J. Mater. Civ. Eng. (ASCE)* **23**:5 (2011), 703–710.
- [Zheng et al. 2015] J.-J. Zheng, J.-G. Dai, and X.-L. Fan, “Fracture analysis of FRP-plated notched concrete beams subjected to three-point bending”, *J. Eng. Mech. (ASCE)* **142**:3 (2015), 1–10.

Received 11 Feb 2019. Revised 21 Apr 2019. Accepted 12 May 2019.

SHAHRIAR SHAHBAZPANAHI: sh.shahbazpanahi@gmail.com

Department of Civil Engineering, Sanandaj Branch, Islamic Azad University, Sanandaj, Iran

HUNAR FARID HAMA ALI: hunar.hamaali@uoh.edu.iq

Department of Building and Construction Engineering, University of Halabja, Kurdistan, Iraq

JOURNAL OF MECHANICS OF MATERIALS AND STRUCTURES

msp.org/jomms

Founded by Charles R. Steele and Marie-Louise Steele

EDITORIAL BOARD

ADAIR R. AGUIAR	University of São Paulo at São Carlos, Brazil
KATIA BERTOLDI	Harvard University, USA
DAVIDE BIGONI	University of Trento, Italy
MAENGHYO CHO	Seoul National University, Korea
HUILING DUAN	Beijing University
YIBIN FU	Keele University, UK
IWONA JASIUK	University of Illinois at Urbana-Champaign, USA
DENNIS KOCHMANN	ETH Zurich
MITSUTOSHI KURODA	Yamagata University, Japan
CHEE W. LIM	City University of Hong Kong
ZISHUN LIU	Xi'an Jiaotong University, China
THOMAS J. PENCE	Michigan State University, USA
GIANNI ROYER-CARFAGNI	Università degli studi di Parma, Italy
DAVID STEIGMANN	University of California at Berkeley, USA
PAUL STEINMANN	Friedrich-Alexander-Universität Erlangen-Nürnberg, Germany
KENJIRO TERADA	Tohoku University, Japan

ADVISORY BOARD

J. P. CARTER	University of Sydney, Australia
D. H. HODGES	Georgia Institute of Technology, USA
J. HUTCHINSON	Harvard University, USA
D. PAMPLONA	Universidade Católica do Rio de Janeiro, Brazil
M. B. RUBIN	Technion, Haifa, Israel

PRODUCTION production@msp.org

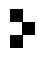
SILVIO LEVY Scientific Editor

See msp.org/jomms for submission guidelines.

JoMMS (ISSN 1559-3959) at Mathematical Sciences Publishers, 798 Evans Hall #6840, c/o University of California, Berkeley, CA 94720-3840, is published in 10 issues a year. The subscription price for 2019 is US \$635/year for the electronic version, and \$795/year (+\$60, if shipping outside the US) for print and electronic. Subscriptions, requests for back issues, and changes of address should be sent to MSP.

JoMMS peer-review and production is managed by EditFLOW[®] from Mathematical Sciences Publishers.

PUBLISHED BY

 **mathematical sciences publishers**
nonprofit scientific publishing

<http://msp.org/>

© 2019 Mathematical Sciences Publishers

Journal of Mechanics of Materials and Structures

Volume 14, No. 3

May 2019

-
- Experimental and numerical energy absorption study of aluminum honeycomb structure filled with graded and nongraded polyurethane foam under in-plane and out-of-plane loading**
ALIREZA MOLAIEE and SEYED ALI GALEHDARI 309
- Transient thermal stresses in a laminated spherical shell of thermoelectric materials**
YUE LIU, KAIFA WANG and BAOLIN WANG 323
- Tuning the propagation characteristics of the trapped and released strongly nonlinear solitary waves in 1-D composite granular chain of spheres**
BIN WU, HEYING WANG, XIUCHENG LIU, MINGZHI LI, ZONGFA LIU and CUNFU HE 343
- Accurate buckling analysis of piezoelectric functionally graded nanotube-reinforced cylindrical shells under combined electro-thermo-mechanical loads**
SHENGBO ZHU, YIWEN NI, JIABIN SUN, ZHENZHEN TONG, ZHENHUAN ZHOU and XINSHENG XU 361
- Thermoelastic fracture initiation: the role of relaxation and convection**
LOUIS M. BROCK 393
- Development of fracture mechanics model of beam retrofitted with CFRP plate subjected to cyclic loading**
SHAHRIAR SHAHBAZPANAH and HUNAR FARID HAMA ALI 413
- Assessment of degradation of railroad rails: finite element analysis of insulated joints and unsupported sleepers**
HOSSAM ELSAYED, MOHAMED LOTFY, HAYTHAM ZOHN and HANY SOBH 429



1559-3959(2019)14:3;1-V